ANALYSIS OF AUTOMOTIVE NEUTRAL GEAR RATTLE

R. Singh, H. Xie and R. J. Comparin

The Ohio State University, Department of Mechanical Engineering, Columbus, Ohio 43210-1107, U.S.A.

(*Received* 22 *February* 1988)

Vibro-impacts induced by backlash between meshing gears lead to excessive vibration and noise in many geared rotating systems. For illustration purposes, a five-speed manual transmission of a front wheel drive automobile is examined, with focus on the neutral gear rattle problem. Several non-linear and linear mathematical models of generic physical systems are developed to understand, quantify and control the problem. A few rattle criteria have been proposed and their application has been demonstrated. Design guidelines for reduced rattle are discussed, and the roles played by the clutch, flywheel and drag torque have been investigated. Results are consistent with those reported in the literature.

1. INTRODUCTION

Backlash exists in all geared systems either by design or due to manufacturing errors and/or wear. Vibro-impacts or rattle, induced by backlash between meshing gears, lead to excessive vibration, noise and dynamic loads in many geared rotating systems such as automotive transmissions and machine tools. The gear rattle problem is more pronounced in essentially unloaded meshes. Therefore, we consider the neutral rattle problem in a five-speed manual transmission of a front wheel drive automobile, shown schematically in Figure 1.

The neutral rattle problem has been modeled by Sakai *et al.* [1], Ohnuma *et al.* [2], and Fujimoto *et al.* [3], and the governing non-linear equations have been solved numerically. Also, several design concepts have been experimentally evaluated [4–9]. Most of these investigations have pointed out the importance of the clutch characteristics [1–3, 5, 8, 9], the drag torque [1, 4], and the flywheel inertia [6–8, 11]. Further, a theory of rattle threshold, based on the comparison of the inertial torque of the driven gear and the drag torque, has been proposed by Seaman *et al.* [4]; it was, in fact, experimentally demonstrated in an earlier work by Sakai *et al.* [1].

It is clear from the available literature [1–11] that either numerical simulation or trial and error type of design/experimental evaluation techniques have been attempted. Consequently, the problem is still poorly understood and an analytical design methodology is not available. The intent of this study is therefore to examine several non-linear and linear models of the neutral rattle problem and to develop suitable rattle criteria. Simple analytical models will be developed to formulate design guidelines for the system, with emphasis on clutch for reduced rattle.

2. PHYSICAL MODEL

Figure 1 shows schematically a generic physical model of an automotive manual transmission. It has been shown by Comparin [12] that this lumped parameter model of four degrees of freedom is sufficient to study the neutral rattle problem; similar models have been used by other investigators [1–3]. The sign convention for the torsional

0022-460X/89/110177+20 $03.00/0

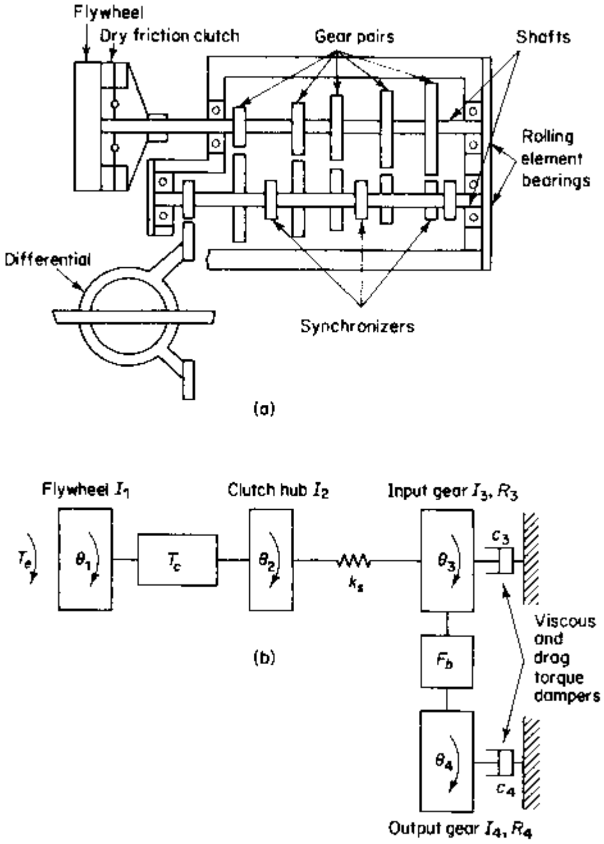

Figure 1. Physical model for the neutral gear rattle problem. (a) Automotive manual transmission schematic; (b) physical model.

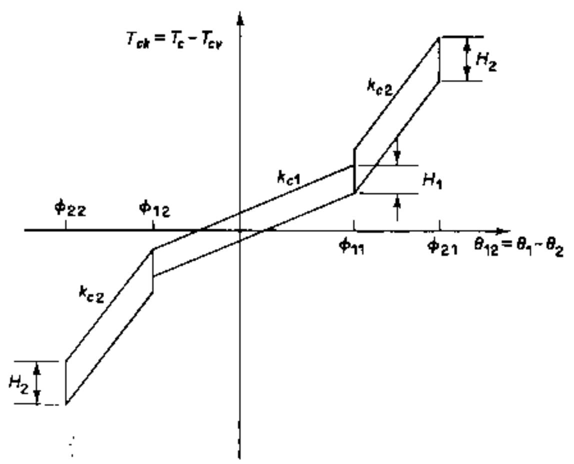

Figure 2. Dynamic characteristics of the clutch. Here $T_{cv} = c_{12}\dot{\theta}_{12}$ is the viscous damping torque, k is the stiffness and H is the hysteresis. This curve is asymmetrical in operational angles (ϕ); i.e., $\phi_{11} \neq \phi_{12}$ and $\phi_{21} \neq \phi_{22}$.

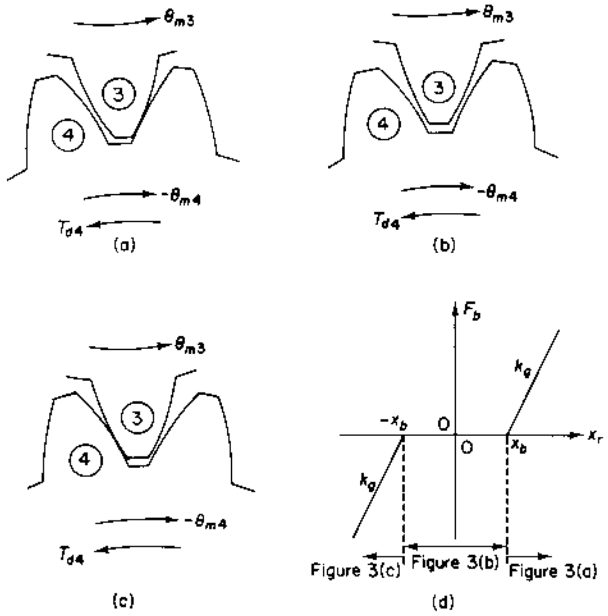

Figure 3. Meshing gears and elastic compression force F_b. (a) Gears in contact on the driving side; (b) gears separated; (c) gears in contact on the driven side; (d) elastic compression force (F_b) with gear teeth meshing stiffness (k_g) and backlash ($2x_b$). Here $x_r = R_3\theta_3 + R_4\theta_4$.

displacements $\theta_i(t) = \theta_{mi}(t) + \theta_{pi}(t)$, $i = 1$–4, is shown in Figure 1, where $\theta_{mi}(t)$ and $\theta_{pi}(t)$ are mean and vibratory parts, respectively. The input gear moment of inertia I_3 also includes the reflected moments of inertia from other gears: i.e., the moments of inertia of all of the input gears and those of the intermediate gears, other than the one used for I_4 calculation, are lumped into one term to yield I_3. Non-linear characteristics of the clutch torque T_c are shown in Figure 2, similar to the curve chosen by Ohnuma *et al.* [2]. The elastic compression force F_b between the conjugate gear pair of radii R_3 and R_4 is given in Figure 3. Here gear meshing stiffness k_g and backlash ($2x_b$) are assumed to be constants, and impact damping is ignored.

3. NON-LINEAR MODEL

The governing equations of motion are given as

$$I_1\ddot{\theta}_1 + T_c = T_e(t), \qquad I_2\ddot{\theta}_2 - T_c + k_s(\theta_2 - \theta_3) = 0, \tag{1, 2}$$

$$I_3\ddot{\theta}_3 - k_s(\theta_2 - \theta_3) + k_g R_3 y(x_r, x_b) = T_{d3}(t), \tag{3a}$$

where

$$T_{d3}(t) = -c_3\dot{\theta}_3(t) = -c_3[\dot{\theta}_{m3} + \dot{\theta}_{p3}(t)], \tag{3b}$$

$$y(x_r, x_b) = \begin{Bmatrix} x_r - x_b, & x_r \geqslant x_b \\ 0{\cdot}0, & -x_b < x_r < x_b \\ x_r + x_b, & x_r \leqslant -x_b \end{Bmatrix}, \qquad x_r = R_3\theta_3 + R_4\theta_4, \tag{3c, d}$$

$$I_4\ddot{\theta}_4 + k_g R_4 y(x_r, x_b) = T_{d4}(t), \tag{4a}$$

where

$$T_{d4} = -c_4\dot{\theta}_4(t) = -c_4[\dot{\theta}_{m4} + \dot{\theta}_{p4}(t)]. \tag{4b}$$

Here y is the dead space function and x_r is the relative displacement between gears. The torque excitation is $T_e(t) = T_m + T_p(t)$, where T_m is the mean part and $T_p(t)$ is the vibratory part. Assuming $T_e(0) = T_m$ and writing a Fourier series expression for $T_p(t)$, one obtains

$$T_e(t) = T_m + \sum_j T_{pj} \sin(\omega_{pj} t + \phi_{pj}), \qquad \omega_{pj} = (N_e/2) j \Omega_e, \qquad j = 1, 2, \ldots, \qquad (5a, b)$$

where N_e is the number of cylinders and Ω_e is engine rotational speed in rad/s. Initial velocities and accelerations are assumed as follows:

$$\dot{\theta}_i(0) = \dot{\theta}_{mi} = \Omega_e, \qquad i = 1, 2, 3, \qquad (6a)$$

$$\dot{\theta}_4(0) = \dot{\theta}_{m4} = -(R_3/R_4)\dot{\theta}_3(0) = -(R_3/R_4)\Omega_e, \qquad (6b)$$

$$\ddot{\theta}_{pi}(0) = 0, \qquad i = 1, 2, 3, 4. \qquad (6c)$$

The initial displacement $\theta_i(0)$ is derived from the static balance of the system as given by the governing equations (1)–(4). Taking $\theta_4(0) = 0$ as the reference, assuming that the balance point ϕ_s for the clutch is between ϕ_{11} and ϕ_{12}, and taking the loading curve in Figure 2 for calculation, one obtains the following, after some manipulation:

$$\theta_1(0) = \frac{T_m - H_1}{k_{c1}} + \frac{T_m}{k_s} + \frac{T_{d4}(0)}{k_g R_3 R_4} + \frac{x_b}{R_3}, \qquad \theta_2(0) = \frac{T_m}{k_s} + \frac{T_{d4}(0)}{k_g R_3 R_4} + \frac{x_b}{R_3}, \qquad (7a, b)$$

$$\theta_3(0) = \frac{T_{d4}(0)}{k_g R_3 R_4} + \frac{x_b}{R_3}, \qquad \phi_{sl} = \theta_1(0) - \theta_2(0) = \frac{T_m - H_1}{k_{c1}}, \qquad (7c, d)$$

$$\phi_{su} = T_m / k_{c1}, \qquad \phi_s = (\phi_{sl} + \phi_{su})/2, \qquad (7e, f)$$

where ϕ_{sl} and ϕ_{su} are the static balance point for loading and unloading, respectively.

4. COMPUTER SIMULATION OF NON-LINEAR MODEL

The non-linear model as given by equations (1)–(7) has been solved numerically using a fixed integration time step (Δt), fourth order Runge–Kutta technique. Since the elastic deformation between the two meshing gears (y) is very small, double precision calculation must be performed in order to ensure accurate simulation. A step size of $\Delta t = 10^{-4}$ s is adequate to simulate the case without any impacts. However, extremely small integration steps, of the order 10^{-6} to 10^{-7} s, are required when the rattle impacts between gears take place; this is due to the fact that the interval between impacts is very small. Still, several problems were encountered in this numerical technique. Some time domain results were not repeatable for different (Δt) and numerical errors were found to accumulate with time as shown later. Higher order Runge–Kutta techniques with variable time steps did not improve the results. Part of the problem was attributed to the stiff differential equations involved which usually require the use of other types of integration techniques such as Gear's method for their solution. This will be the subject of a future paper.

Although other investigators also have used Runge–Kutta techniques [1–3], numerical difficulties have not been discussed. Hence, some of the available data may be suspect. Overall, it is clear that the numerical simulation technique for the gear rattle problem can be error-prone and time-consuming for parametric studies. Consequently, linear analytical or simple non-linear models must be employed.

5. LINEAR MODEL

The linearized equations are derived on the basis of the following assumptions: (i) small vibratory amplitudes; (ii) only the first stage of the clutch is active, i.e., $\phi_{12} < \theta_{12} < \phi_{11}$; (iii) $H_1 = c_{12} = 0$; (iv) gear teeth remain in contact on the driving side, as shown in Figure 3(a); (v) constant drag torques, i.e., $T_{d3} = -c_3\dot{\theta}_{m3}$, and $T_{d4} = -c_4\dot{\theta}_{m4}$, as $|\dot{\theta}_m| \gg |\dot{\theta}_p|$. Redefining the co-ordinate system as $\theta_i'(t) = \theta_i(t) - \theta_{mi}(t) - \theta_i(0) = \theta_{pi}(t) - \theta_i(0)$, $i = 1$-4, one obtains the following equations in the matrix form (this procedure eliminates mean and drag torque terms and sets the initial conditions to zero):

$$[M]\{\ddot{\theta}'(t)\} + [K]\{\theta'(t)\} = \{T(t)\}. \tag{8a}$$

Here

$$\{\theta'(t)\}^{\mathrm{T}} = [\theta_1'(t), \theta_2'(t), \theta_3'(t), \theta_4'(t)], \qquad \{T(t)\}^{\mathrm{T}} = [T_p(t), 0, 0, 0], \tag{8b, c}$$

$$[M] = \begin{bmatrix} I_1 & 0 & 0 & 0 \\ 0 & I_2 & 0 & 0 \\ 0 & 0 & I_3 & 0 \\ 0 & 0 & 0 & I_4 \end{bmatrix}, \; [K] = \begin{bmatrix} k_{c1} & -k_{c1} & 0 & 0 \\ -k_{c1} & k_{c1} + k_s & -k_s & 0 \\ 0 & -k_s & k_s + k_g R_3^2 & k_g R_3 R_4 \\ 0 & 0 & k_g R_3 R_4 & k_g R_4^2 \end{bmatrix}. \tag{8d, e}$$

An eigensolution of equation (8) yields natural frequencies ω_r, $r = 2$-4 (with $\omega_1 = 0$) and normal modes $\{\psi\}_r$. The analytical solution based on the normal mode method when the excitation is assumed as $T_p(t) = T_{p1} \sin(\omega_{p1} t) + T_{p2} \sin(\omega_{p2} t)$ is

$$\begin{aligned} \{\theta'(t)\} &= [\psi]\{\eta(t)\} \\ &= \{P_{p1}\} \sin(\omega_{p1} t) + \{P_{p2}\} \sin(\omega_{p2} t) + \{\{P_1\} t + \sum_{r=2}^{4} \{P_r\} \sin(\omega_r t), \end{aligned} \tag{9}$$

where $\eta(t)$ is the normal co-ordinate and P_p and P are the participation factors corresponding to forced and free vibrations, respectively.

6. RATTLE CRITERIA

6.1. CRITERION BASED ON RELATIVE DISPLACEMENT BETWEEN GEARS (x_r)

Vibro-impacts or rattle should not occur when the gears remain in contact at the driving side, as shown in Figure 3(a); this implies that $x_r(t) \geqslant x_b$. Rattle between conjugate gears will obviously take place under the following conditions: (i) gears are separated and free to move within the backlash as shown in Figure 3(b), and (ii) the gears are in contact on the driven side as shown in Figure 3(c)—since this case is not compatible with the mean torque requirements, separation will occur very quickly; consequently, Figure 3(c) is an unstable case and must be avoided. Mathematically, a rattle criterion can be given in terms of $x_r(t)$ as

$$x_r(t) \left\{ \begin{matrix} < x_b: & \text{rattle} \\ \geqslant x_b: & \text{no rattle} \end{matrix} \right\}. \tag{10a, b}$$

6.2. CRITERION BASED ON ANGULAR ACCELERATION OF OUTPUT GEAR ($\ddot{\theta}_4$)

By using Equations (3c), (4a) and (10), and noting that $T_{d4} - I_4\ddot{\theta}_4 > 0$ is equivalent to $x_r(t) - x_b > 0$, but $T_{d4} - I_4\ddot{\theta}_4 = 0$ is not equivalent to $x_r(t) - x_b = 0$, the rattle criterion can be reformulated as

$$T_{d4} - I_4\ddot{\theta}_4(t) \left\{ \begin{matrix} \leqslant 0: & \text{rattle} \\ > 0: & \text{no rattle} \end{matrix} \right\}. \tag{11a, b}$$

This implies that the drag torque be sufficient to overcome the inertial torque to ensure rattle-free transmission. Equation (11) is in fact that of the Seaman *et al.* rattle threshold theory [4], which is based on a single gear pair analysis with the assumption of a constant drag torque on the driven gear. Earlier, Sakai *et al.* [1] had measured the increase in rattle noise ΔL_N (in dB) for a single input and counter gear pair. The measurement indicated that $\Delta L_N = 0$ dB when $I_r\ddot{\theta}_4/T_{d4} < 1$, which is consistent with equation (11b). When $I_4\ddot{\theta}_4/T_{d4}$ was varied from 1 to 10, ΔL_N increased by 0 to 4·6 dB, as predicted by equation (11b); however, they did not establish a criterion or rattle level index. But, it should be noted that $\ddot{\theta}_4(t)$ and $T_{d4}(t)$ are difficult to calculate when the rattle occurs, as discussed in section 4.

6.3. CRITERION BASED ON ANGULAR ACCELERATION OF INPUT GEAR

We now propose a new rattle criterion based on $\ddot{\theta}_3(t)$. When the gears are in contact, the elastic deformation is very small and therefore one can approximate $\ddot{\theta}_4(t)$ as

$$\ddot{\theta}_4(t) = -(R_3/R_4)\ddot{\theta}_3(t). \tag{12}$$

Using equations (11) and (12), one can define the approximate rattle level time history as

$$\beta(t) \simeq (I_4 R_3/T_{d4} R_4)\ddot{\theta}_3(t), \tag{13}$$

Hence the rattle criterion is approximately given as

$$\beta(t)\begin{Bmatrix} \leqslant -1: & \text{rattle} \\ > -1: & \text{no rattle} \end{Bmatrix}. \tag{14a, b}$$

Equation (14b) for the no rattle case does not restrict the absolute value of $\ddot{\theta}_3(t)$, which may be substantial. In order to restrict this absolute motion for the rattle-free case, the rattle criterion is modified as

$$|\beta(t)|\begin{Bmatrix} \geqslant 1: & \text{rattle} \\ < 1: & \text{no rattle} \end{Bmatrix}. \tag{15a, b}$$

It should be noted that $|\beta(t)|$ calculation based on $\ddot{\theta}_3(t)$ is an approximate one: however, it is easier to compute and more reliable as is to be demonstrated later.

For a practical gearbox, x_b and T_{d4} may not be constants, and the $\ddot{\theta}_3(t)$ signature may be fairly complicated. Hence, it is more convenient to calculate the root-mean-square (r.m.s.) value, β_{rms}, which is related to the energy contents of the motion. Assuming a harmonic relationship for $\ddot{\theta}_3(t)$, one obtains the criterion

$$\beta_{rms}\begin{Bmatrix} \geqslant 0{\cdot}707: & \text{rattle} \\ < 0{\cdot}707: & \text{no rattle} \end{Bmatrix}, \tag{16a, b}$$

where

$$\beta_{rms} = \frac{1}{T}\int_0^T \beta^2(t)\,\mathrm{d}t, \qquad T = \text{time window}. \tag{16c}$$

The rattle level L_β (in dB) and the corresponding rattle criterion are defined as follows (this formulation should also be useful for experimental work):

$$L_\beta = 20\log_{10}(\beta_{rms}/0{\cdot}707) \quad \text{dB}, \tag{17a}$$

$$L_\beta\begin{Bmatrix} \geqslant 0\ \text{dB}: & \text{rattle} \\ < 0\ \text{dB}: & \text{no rattle} \end{Bmatrix}. \tag{17b, c}$$

7. RESULTS

Table 1 summarizes four example cases which correlate computer simulation predictions with rattle criteria. Numerical values of various parameters are given in section 9.1.

TABLE 1

Computer simulation results and rattle levels

	Case			
	I	II	III	IV
T_{d4}	$T_{d4} \neq T_{d4}(t)$	$T_{d4}(t)$	$T_{d4}(t)$	$T_{d4}(t)$
x_b (mm)	0·075	0·075	0·075	0·075
$\bar{x}_r$ = mean x_r (mm)	0·075	0·075	0·025	0·036
y_{rms} (mm) $\times 10^{-6}$	2·62	2·58	38·0	33·9
θ_{12rms} (degrees)	2·09	2·00	0·483	0·482
$\ddot{\theta}_{2rms}$ (rad/s^2)	11·2	8·41	180·0	179·0
$\ddot{\theta}_{3rms}$ (rad/s^2)	11·2	8·41	172·0	170·0
$\ddot{\theta}_{4rms} \times (R_4/R_3)$ (rad/s^2)	11·2	8·41	573·0	511·0
L_β (dB)	−7·52	−10·1	16·1	16·0
Corresponding figures	4, 5	6	7, 8	7, 8

7.1. CASE I: LINEAR MODEL

This case follows all of the assumptions made in section 5 for the four-degree-of-freedom linear system model. Figures 4(a) and (b) present the $\ddot{\theta}_3(t)$ which were predicted by the linear model and the computer simulation (non-linear model), respectively; we note excellent correlation. Similar comparisons have been found for other time histories including $\theta_{12}(t)$ and $x_r(t)$. Figure 5(a) shows $\beta(t)$ for this case; it can be shown that

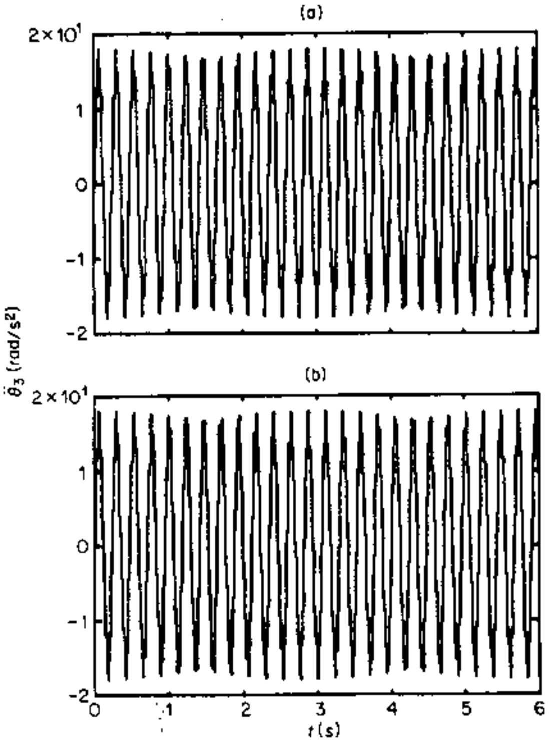

Figure 4. Input gear acceleration for Case I. (a) Linear model; (b) computer simulation (non-linear model). $\ddot{\theta}_{3rms} = 11{\cdot}2$ (rad/s^2).

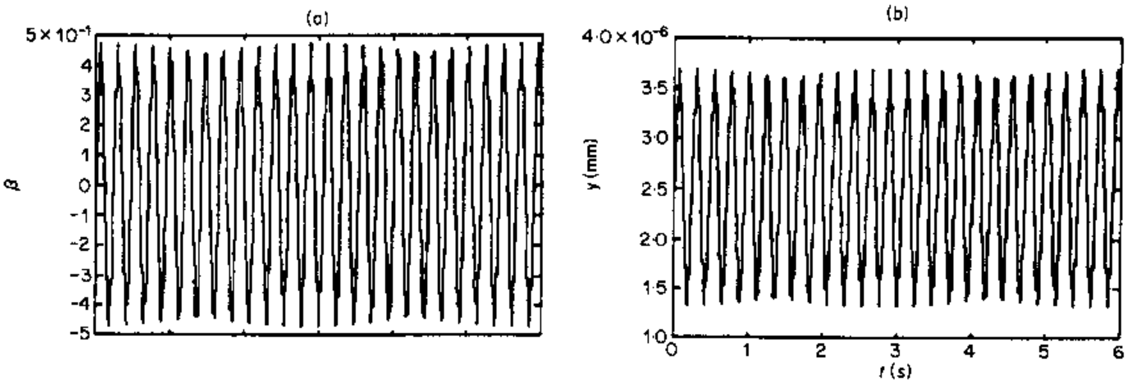

Figure 5. Computer simulation predictions for Case I. (a) Rattle level $\beta(t)$, $\beta_{rms}=0{\cdot}297$; (b) Relative deflection between gear teeth given by $y(t)=x_r(t)-x_b$; $y_{rms}=2{\cdot}62\times10^{-6}$ (mm).

$|\beta(t)|<0{\cdot}5$ and $L_\beta=-7{\cdot}5$ dB. This corresponds to the rattle criteria given by equations (15a) and (17a) which predict that rattle will not take place. This is in fact the case, as $x_r=x_b+y$ since $0\leqslant y(t)\ll 1$; this is shown in Figure 5(b) where $|y(t)|<4\times10^{-6}$ mm.

7.2. CASE II: VARIABLE DRAG TORQUE

One can now add variable drag torque terms $T_{d3}(t)$ and $T_{d4}(t)$ through viscous dampers to the linear model of Case I. This is simulated here only numerically. Like Case I, the rattle criteria are satisfied as $x_r=x_b+y$ since $0\leqslant y(t)\ll 1$ and $|\beta(t)|<1$. The rattle level for Case II, as given in Table 1, is lower than the level seen for Case I. This is because of the viscous damping effects shown in Figure 6 for $\beta(t)$.

7.3. CASES III AND IV: RATTLE PHENOMENON AND EFFECT OF INTEGRATION STEP (Δt)

Figure 7 presents $x_r(t)$ when rattle takes place; Figure 7(a) corresponds to $\Delta t=5\times10^{-7}$ s (Case III), and Figure 7(b) gives results for $\Delta t=2{\cdot}5\times10^{-7}$ s (Case IV). One can note differences in not only the time history but in r.m.s. values as well. Further, Table 1 shows a large difference in θ_{4rms} values for these two steps. However, $\ddot{\theta}_{3rms}$ and L_β as given in Table 1, and $\theta_{12}(t)$ as given in Figure 8, are not sensitive to the choice of Δt as long as Δt is of the order of 10^{-6} s. This illustrates that the computations of $\theta_1(t)$, $\theta_2(t)$ and $\ddot{\theta}_{3rms}$

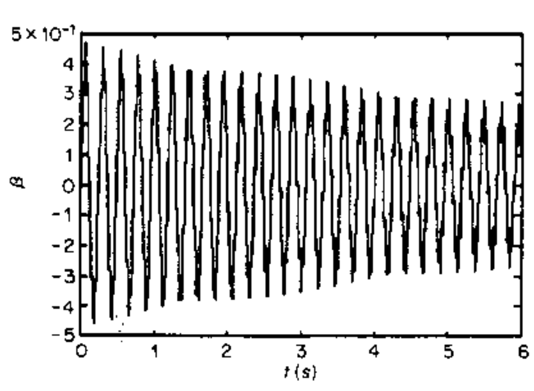

Figure 6. Computer simulation predictions of rattle level $\beta(t)$ for Case II. $\beta_{rms}=0{\cdot}221$.

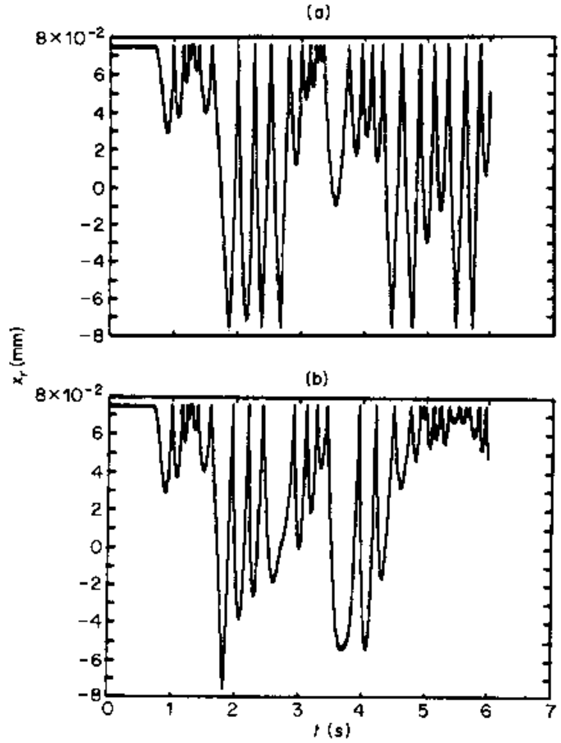

Figure 7. Relative displacement between gears $x_r(t)$ when rattle takes place. (a) $\Delta t = 5{\cdot}0\times10^{-7}$ s (Case III), $x_{rrms} = 5{\cdot}05\times10^{-2}$ (mm); (b) $\Delta t = 2{\cdot}5\times10^{-7}$ s (Case IV), $x_{rrms} = 5{\cdot}32\times10^{-2}$ (mm).

are fairly accurate; conversely, accurate results for $\theta_3(t)$, $\theta_4(t)$, θ_{4rms} and $x_r(t)$ are difficult to obtain, as discussed earlier in section 4. Accordingly, $\ddot{\theta}_{3rms}$ is the most appropriate quantity which can be related to the rattle criterion, as explained previously in section 6.

8. SIMPLIFIED PHYSICAL MODEL AND DESIGN GUIDELINES

8.1. JUSTIFICATION AND GOVERNING EQUATIONS

Table 2 compares modal participation factors associated with the accelerations for both forced and free vibrations. They have been obtained by using the four-degree-of-freedom linear model given by equation (9). From this data for the rattle free case, i.e., $|\beta(t)| < 1$, it is clear that there is very little relative motion between the clutch hub, the input gear and the intermediate gear. Also, the modal participation factors for the third and the fourth modes are extremely small. Accordingly, equation (9) can be simplified as follows (and the linear system is reduced to a two-degree-of-freedom system):

$$\{\theta'(t)\} = \{P_{p1}\}\sin(\omega_{p1}t) + \{P_{p2}\}\sin(\omega_{p2}t) + \{P_1\}t + \{P_2\}\sin(\omega_2 t), \tag{18a}$$

$$\begin{aligned}\{\theta'(t)\}^{\mathrm{T}} &= [\theta_1'(t), \theta_2'(t), \theta_3'(t), \theta_4'(t)]\\ &= [\theta_1'(t), \theta_2'(t), \theta_2'(t), -(R_3/R_4)\theta_2'(t)].\end{aligned} \tag{18b}$$

Further, from Table 1 one can note for the rattle-free cases (I and II) that the non-linear simulation model also predicts that $\ddot{\theta}_{2rms} = \ddot{\theta}_{3rms} = (R_4/R_3)\ddot{\theta}_{4rms}$. Accordingly, one can reduce the physical model of Figure 1 to a two-degree-of-freedom, non-linear model as

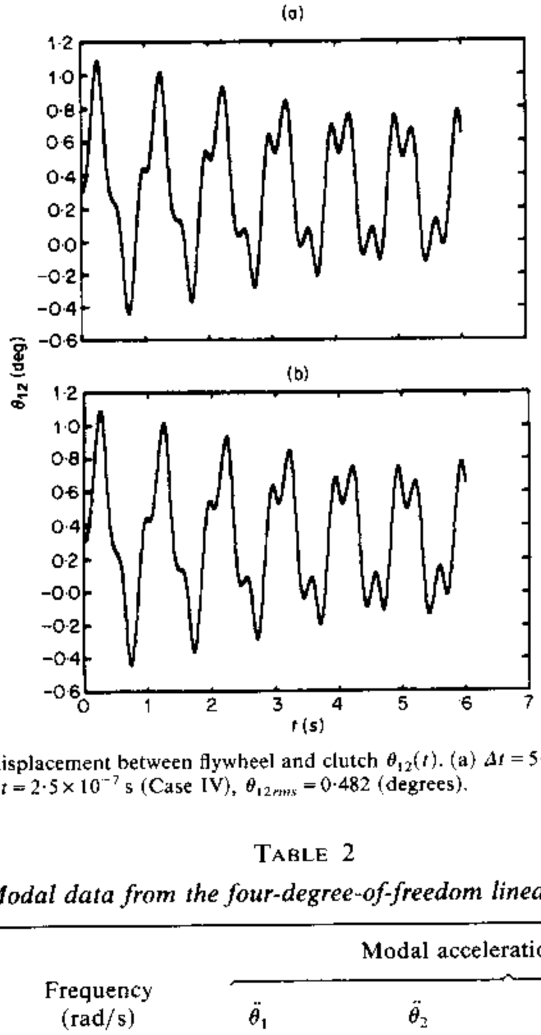

Figure 8. Relative displacement between flywheel and clutch $\theta_{12}(t)$. (a) $\Delta t = 5\cdot0\times10^{-7}$ s (Case III), $\theta_{12rms} = 0\cdot483$ (degrees); (b) $\Delta t = 2\cdot5\times10^{-7}$ s (Case IV), $\theta_{12rms} = 0\cdot482$ (degrees).

TABLE 2

Modal data from the four-degree-of-freedom linear model

	Frequency (rad/s)	Modal accelerations (rad/s²)			
		$\ddot{\theta}_1$	$\ddot{\theta}_2$	$\ddot{\theta}_3$	$-\frac{R_4}{R_3}\ddot{\theta}_4$
Forced vibration	$\omega_{p1} = 188\cdot5$	102·0	−13·2	−13·3	−13·3
	$\omega_{p2} = 377\cdot0$	25·5	−0·733	−0·764	−0·764
Free vibration	$\omega_1 = 0\cdot0$	0·0	0·0	0·0	0·0
	$\omega_2 = 65\cdot2$	−1·96	42·6	42·6	42·6
	$\omega_3 = 2\,804\cdot9$	$1\cdot54\times10^{-7}$	$-6\cdot44\times10^{-3}$	$5\cdot34\times10^{-3}$	$5\cdot46\times10^{-3}$
	$\omega_4 = 19\,946\cdot0$	$1\cdot48\times10^{-16}$	$-3\cdot14\times10^{-10}$	$2\cdot88\times10^{-8}$	$-2\cdot97\times10^{-7}$

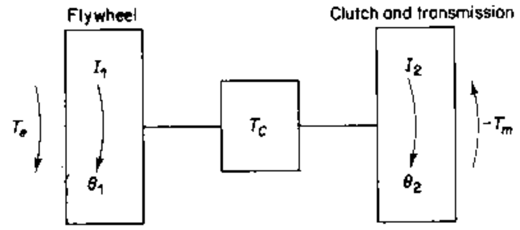

Figure 9. Simplified physical model for the neutral gear rattle problem.

shown in Figure 9. Here, the effective value of I_2 includes inertia of the transmission beyond the clutch spring: i.e.,

$$(I_2)_{effective} = (I_2)_{clutch} + I_3 + (R_3/R_4)^2 I_4. \tag{19}$$

The governing equations are now given as follows (here T_c and T_e are still defined by Figure 2 and equation (5), respectively):

$$I_1\ddot{\theta}_1 + T_c = T_m + T_p(t), \qquad I_2\ddot{\theta}_2 - T_c = -T_m. \tag{20a, b}$$

From the static balance, initial conditions are now

$$\dot{\theta}_1(0) = \dot{\theta}_2(0) = \dot{\theta}_{m1} = \dot{\theta}_{m2} = \Omega_e, \tag{21a}$$

$$\theta_2(0) = 0, \qquad \theta_1(0) = (T_m - H_1)/k_{11} = \phi_{st}. \tag{21b}$$

8.2. EQUIVALENT LINEAR MODEL

The computer simulation program discussed earlier in section 4 for the four-degree-of-freedom non-linear system can be easily adapted to the two-degree non-linear system of Figure 9. Additionally, one can linearize the system and find an approximate harmonic solution based on the following assumptions: (i) excitation torque is given by $T_p(t) = |T_p|\,\mathrm{e}^{\mathrm{i}\omega_p t}$; (ii) response exists only at ω_p as subharmonics and superharmonics of ω_p are ignored; (iii) only the first stage of the clutch is active, i.e., $\phi_{12} < \theta_{12} < \phi_{11}$; (iv) hysteresis of the first stage, H_1, is negligible (typically the case in a real-life clutch). The clutch torque T_c is

$$\begin{aligned} T_c &= k_{c1}\theta_{12} + c_{12}\dot{\theta}_{12} \\ &= k_{c1}(\theta_r + \phi_{st}) + c_{12}\dot{\theta}_r = k_{c1}\theta_r + c_{12}\dot{\theta}_r + T_m, \end{aligned} \tag{22a}$$

where

$$\theta_r(t) = \theta_1'(t) - \theta_2'(t) = \theta_{12}(t) - \phi_{st}. \tag{22b}$$

Using equations (20) and (22), and the assumptions gives the resulting equations as one for a single-degree-of-freedom system in terms of θ_r; this is obvious as the two-degree-of-freedom system is a semi-definite system:

$$\ddot{\theta}_r + 2\zeta_2\omega_2\dot{\theta}_r + \omega_2^2\theta_r = (|T_p|/I_1)\,\mathrm{e}^{\mathrm{i}\omega_p t}. \tag{23a}$$

Here

$$\omega_2 = \sqrt{k_{c1}\left(\frac{1}{I_1} + \frac{1}{I_2}\right)}, \qquad \zeta_2 = \frac{c_1}{2\sqrt{k_{c1}[I_1 I_2/(I_1 + I_2)]}}. \tag{23b, c}$$

The harmonic response is

$$\frac{I_1|\ddot{\theta}_r|}{|T_p|} = \frac{I_1|\ddot{\theta}_1 - \ddot{\theta}_2|}{|T_p|} = R_a(r, \zeta) = \frac{r^2}{\sqrt{(1-r^2)^2 + (2\zeta r)^2}}, \qquad r = \omega_p/\omega_2, \tag{24}$$

Where R_a is the dynamic magnification factor for $|\ddot{\theta}_r| = \omega_p^2|\theta_r|$—see reference [13], p. 43, for a typical plot. Using equations (20), (22) and (23), one obtains

$$\ddot{\theta}_2 = \ddot{\theta}_2' = (1/I_2)[k_{c1}\theta_r + c_{12}\dot{\theta}_r] = (1/I_2)\tilde{k}_{c1}\theta_r, \tag{25a}$$

where

$$\tilde{k}_{c1} = k_{c1} + \mathrm{i}\omega_p c_{12}, \tag{25b}$$

and

$$|\ddot{\theta}_2| = |\tilde{k}_{c1}||\theta_r|/I_2 = [|T_p|/(I_1 + I_2)]R_T, \tag{26a}$$

where

$$R_T = \sqrt{1+(2\zeta r)^2}/\sqrt{(1-r^2)^2+(2\zeta r)^2}. \tag{26b}$$

Here, R_T is the dimensionless force or motion transmissibility for a single-degree-of-freedom system—see reference [13], p. 95, for a typical plot.

8.3. TRANSMISSIBILITY AND DESIGN GUIDELINES

From equations (13), (15a) and (26), and noting that $T_{d4} = -c_4\dot{\theta}_{m4} = c_4(R_3/R_4)\Omega_e$, the rattle criterion can now be related to R_T. For the rattle-free case

$$|\beta(t)| = \frac{I_4 R_3}{T_{d4} R_4}|\ddot{\theta}_2| = \frac{I_4|T_p|}{c_4\Omega_e(I_1+I_2)} R_T < 1,$$

or

$$R_T < \{(c_4\Omega_e/|T_p|)[(I_1+I_2)/I_4]\}. \tag{27}$$

From a typical R_T curve [13], one knows that $r = \omega_p/\omega_2$ should be greater than $\sqrt{2}$, and ζ_2 should be kept as low as possible. The natural frequency ω_2 can be easily altered by changing clutch stiffness k_{c1}; for low transmissibility across the clutch, k_{c1} should be as low as possible [1–3]. Additionally, one can note from equation (27) the following desirable conditions for the rattle-free case: (i) higher c_4 and engine idling speed Ω_e to yield large T_{d4}—this has been discussed by Sakai *et al.* [1] and Seaman *et al.* [4]; (ii) very small $|T_p|$—this is intuitively obvious; (iii) very large flywheel and clutch inertia (I_1+I_2) compared to the intermediate gear I_4—this is in agreement with results of Ohnuma *et al.* [2] and Fudala *et al.* [11]. Thus one finds that equation (27) gives several design guidelines, and is consistent with the experimental and numerical findings in the literature [1, 2, 4, 11].

8.4. A DESIGN CASE—DUAL MASS FLYWHEEL CONCEPT

Figure 10(a) shows schematically a flywheel design [6–8] which consists of two inertia elements I_a and I_b joined by a spring of stiffness k_f. Here, only the simplified linear system consisting of flywheel and clutch is used in order to demonstrate the feasibility of design for reduced rattle using the linear system theory. This system can be reduced to a two-degree-of-freedom system of Figure 8, as shown in Figure 10(b), provided that the following parameters are chosen: $k_f \leq 0{\cdot}5k_c$, $I_2 \leq 0{\cdot}05 I_1$, $I_1 = I_a + I_b$ and $I_a \simeq I_b \simeq 0{\cdot}5 I_1$.

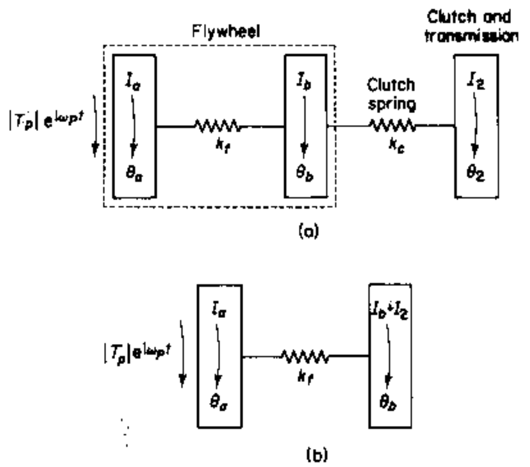

Figure 10. Dual mass flywheel concept. (a) Physical model; here only flywheel-clutch system is shown and all elements are considered linear; (b) simplified model of the system.

Hence, equation (23a) can be rewritten for the undamped case as

$$\ddot{\theta}_r + \omega_2^2\theta_r = (|T_p|/I_1)\, e^{i\omega_p t}, \tag{28a}$$

where

$$\theta_r = \theta_a - \theta_b, \qquad \omega_2 = \sqrt{k_c\left[\frac{1}{I_1} + \left(\frac{1}{I_b + I_2}\right)\right]}. \tag{28b, c}$$

In section 8.2, it has already been shown for the rattle-free case that one needs to keep ω_2 as low as possible. From equation (28c), one knows that this condition is satisfied when $I_a = I_b + I_2 = 0{\cdot}5 \times I_t$, where $I_t = I_a + I_b + I_2 = I_1 + I_2$. Therefore, the minimum value of ω_2 is equal to $2\sqrt{k_f/I_t}$. This is in agreement with the results reported in the literature [6, 8]. Upon using equation (5b), the resonance condition for this $(\omega_2)_{min}$ is found to be

$$\omega_p/(\omega_2)_{min} = (N_e\Omega_e/4)\sqrt{I_t}/k_f = 1. \tag{29}$$

Accordingly, the critical flywheel stiffness that must be avoided is

$$(k_f)_{critical} = \tfrac{1}{16}N_e^2\Omega_e^2 I_t. \tag{30}$$

Table 3 compares $(k_f)_{critical}$ values calculated by using equation (30) with those read from the design curve given by Drexl *et al.* [8]. In order to ensure a rattle-free case, one should set $k_f < 0{\cdot}5 \times (k_f)_{critical}$ corresponding to $\omega_p > \sqrt{2}\omega_2$. Also, k_f and I_t should be chosen such that equation (27) is satisfied.

TABLE 3

Dual mass flywheel system critical stiffness $(k_f)_{critical}$

	$\Omega_e \times (60/2\pi)$ (rpm)		$(k_f)_{critical} \times (2\pi/360)$ (Nm/degree)	
I_t (kg m^2)	$N_e = 4$	$N_e = 6$	Equation (30)	Literature [8]
0·15	400	267	4·59	4·5
0·15	600	400	10·34	10·6
0·15	800	533	18·37	17·9
0·15	1000	667	28·71	28·4
0·20	400	267	6·12	6·1
0·20	600	400	13·78	14·2
0·20	800	533	24·49	24·2

9. CLUTCH DESIGN STUDIES

9.1. PHYSICAL EXAMPLE

For parametric studies, a five-speed manual transmission gearbox, with the following parameters, for a front wheel drive automobile, has been examined: $I_1 = 0{\cdot}16$ kgm^2, $I_2 = 3{\cdot}35 \times 10^{-3}$ kgm^2, $R_3 = 24{\cdot}0$ mm, $I_3 = 3{\cdot}68 \times 10^{-3}$ kgm^2, $R_4 = 50{\cdot}0$ mm, $I_4 = 1{\cdot}53 \times 10^{-3}$ kgm^2, $k_s = 1{\cdot}44 \times 10^4$ Nm/rad, $k_g = 2{\cdot}22 \times 10^8$ N/m, $c_3 = 1{\cdot}57 \times 10^{-4}$ Nm/(rad/s), $c_4 = 0{\cdot}68 \times 10^{-4}$ Nm/(rad/s); T_{d3} and T_{d4} are constants calculated by using assumption (v) made in section 5. Since the emphasis is on the clutch design, various clutch parameters given in Figure 2 will be selected based on the analysis.

For this design study, the simplified model of Figure 8 is used. The analytical modeling technique for a linear clutch and the computer simulation technique for a non-linear clutch are employed. The excitation torque T_e for this case, based on a typical engine torque history, is assumed to be given by the first two harmonics for a four cylinder case at 900 rpm ($\Omega_e = 94{\cdot}25$ rad/s): $T_e(t) = T_m + T_p(t)$ and $T_p(t) = 16{\cdot}297 \sin(\omega_p t) + 4{\cdot}07425 \sin(2\omega_p t)$ Nm, where $\omega_p = 2\Omega_e = 188{\cdot}5$ rad/s. The rattle levels $\beta(t)$ and L_β given by equation (15) and (17) are modified based on the $\ddot{\theta}_2$ calculation:

$$\beta^*(t) = \frac{I_4 R_3}{T_{d4} R_4}\,\ddot{\theta}_2(t) = \frac{I_4}{c_4 \Omega_e}\,\ddot{\theta}_2(t), \qquad L_{\beta^*} = 20\log_{10}(\beta^*_{rms}/0{\cdot}707). \qquad (31\text{a, b})$$

For the rattle-free case, $\beta^*(t) = \beta(t)$, but $\beta^*(t) \neq \beta(t)$ when the rattle takes place as $\ddot{\theta}_2(t) \neq \ddot{\theta}_3(t)$. However, $\beta^*(t)$ is used here for computational ease, and it should be valid for clutch parametric studies. The key is to keep $\beta^*(t)$ and L_{β^*} as low as possible when the rattle takes place. For final calculations, $\beta(t)$ from equation (13) must be computed for verification.

9.2. FIRST STAGE

The design of the first stage clutch spring k_{c1} is based on the following assumptions: (i) $\phi_{11} \to \infty$, $\phi_{12} \to -\infty$, (ii) $c_{12} = 0$ and $H_1 = 0$; (iii) $|T_{p1}| = 16{\cdot}297$ Nm as given in section 9.1. Using equation (27) for the parameters chosen, one finds that $R_T < 0{\cdot}388$. For the undamped case, this corresponds to $r > 1{\cdot}90$, or $r = \omega_p/\omega_2 = 2\Omega_e/\omega_2 = 188{\cdot}5/\omega_2 > 1{\cdot}90$. Hence the natural frequency $\omega_2 < 99{\cdot}2$ rad/s, but this value is too close to the engine rotational speed $\Omega_e = 94{\cdot}25$ rad/s, which could cause resonance problems. Therefore, we chose $\Omega_e/\omega_2 > \sqrt{2}$ from the isolation criterion. This yields $\omega_2 < 66{\cdot}63$ rad/s and $k_{c1} < 31$ Nm/rad. For $k_{c1} = 30$ Nm/rad, a numerical simulation of this system was carried out which included free and forced vibration terms. The computed $\beta^*(t)$ is given in Figure 11(a). One can note that $|\beta^*(t)| > 1$, which implies that the rattle will occur. Hence, a much smaller k_{c1} should be chosen, say $k_{c1} = 5$ Nm/rad. The numerically predicted $\beta^*(t)$ is given in Figure 11(b); now one can note that $|\beta^*(t)| < 0{\cdot}5$ which ensures the rattle-free case. This prediction for a two-degree-of-freedom system case agrees well with the numerical simulation of the four-degree-of-freedom system reported earlier in Figure 5(a) for $\beta(t)$—under Case I with the parameters listed in section 9.1 and $k_{c1} = 5$ Nm/rad.

Decreasing k_{c1} from 30 to 5 Nm/rad increases the operational angle of the clutch θ_{12rms} from 0·54° with static balance point $\phi_s = 0{\cdot}31°$ to $\theta_{12rms} = 2{\cdot}09°$ with $\phi_s = 1{\cdot}8°$, as evident from Table 4. While the rattle problem has been solved by choosing a compliant spring, higher clutch operational angles θ_{12} and balance points ϕ_s are obtained. Both of these could force the clutch operational angle to move into the second stage, past ϕ_{11} and/or ϕ_{12}. This transition could cause a severe rattle problem as discussed later in section 9.3.

Since the static balance point ϕ_s is related to the hysteresis H_1, higher H_1 is required to keep ϕ_s low. This should also decrease $\theta_{12}(t)$ and $\beta^*(t)$ as free vibrations would be damped out, as illustrated by Table 4. The effect of increasing c_{12} on θ_{12} and $\beta^*(t)$ is similar except that ϕ_s is not affected by c_{12}. Hence, one can design a combination of H_1 and c_{12} which in practice would be obtained by hysteresis and contact friction. One word of caution: from the transmissibility point of view, higher damping tends to increase the amplitude of the forced vibration in the isolation range; this can be seen from Table 4. Hence, an optimal value of H_1 must be selected; for example, H_1 should be of the order of 0·05 Nm from Table 4.

9.3. DUAL STAGE CLUTCH AND TRANSITION PHENOMENON

One can now consider the dual stage clutch as shown in Figure 2 and examine the effects of various design parameters using the computer simulation program. It should be noted that k_{c2} is primarily selected on the basis of the mean power requirements. Table 5, which gives results for the dual stage clutch, should also be compared with Table 4

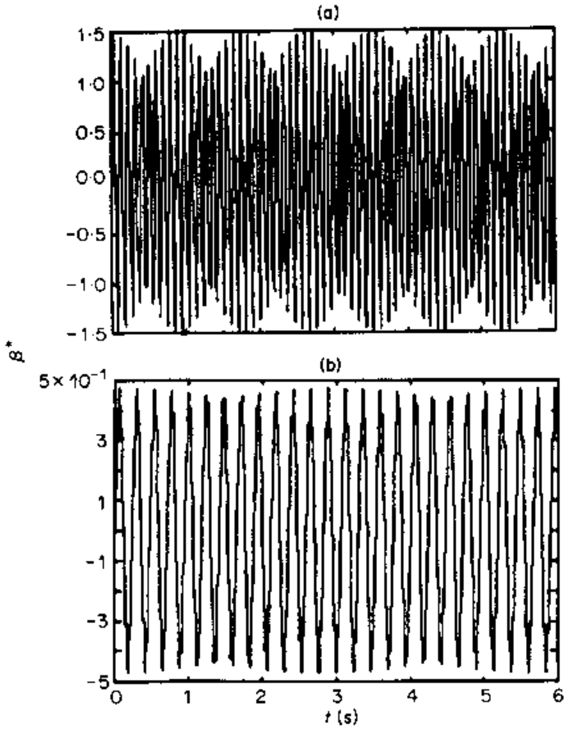

Figure 11. Numerical simulation of the simplified system with linear clutch (see section 4.1). (a) k_{c1} = 30·0 Nm/rad, $\beta^*_{rms} = 0{\cdot}835$; (b) $k_{c1} = 5{\cdot}0$ Nm/rad, $\beta^*_{rms} = 0{\cdot}297$.

given for the single stage clutch. First, it is assumed that the dual stage is available only on the driving side: i.e., ϕ_{11} is limited and set close to ϕ_s and ϕ_{12} is unlimited, as given in Table 5(a). Once the motion is initiated, the clutch quickly moves into the second stage of higher stiffness k_{c2} and back to the first stage of lower stiffness k_{c1} at a rapid rate, as shown in Figure 12(a). The stiffness transition at ϕ_{12} increases L_{β^*} by 10–20 dB, as shown in Table 5. This can be explained partially from the transmissibility discussion given in sections 8.2 and 9.2, which predicted rattle for a higher stiffness value as encountered here in k_{c2}. This phenomenon has also been discussed in the literature [2, 3, 5], where it is called as the "jumping" or "bump" phenomenon. Further analytical investigation is required to understand the effects of the transition phenomenon. At this point one can, however, conclude the following based on the numerical results given in Table 5: (i) the transition phenomena at both sides is much worse than the one-sided transition as L_{β^*} increases by approximately 20 dB—see Figure 12(b) and Table 5(a); (ii) a smaller k_{c2}/k_{c1} ratio gives lower L_{β^*}, (iii) a dual stage clutch of fairly low k_{c1} and k_{c2} values is comparable to a single stage clutch; (iv) the asymmetric nature of the clutch as dictated by H_1, H_2 and T_{d3} may be desirable to reduce the rattle level associated with the transition phenomenon; (v) the mean value of the relative displacement $\bar{\theta}_{12}$ is not equal to ϕ_s, unlike for the single stage; (vi) higher H_1 and H_2 values are not necessarily better as optimal values must be chosen while controlling ϕ_s; (vii) an increase in c_{12} reduces L_{β^*}.

9.4. DESIGN GUIDELINES

On the basis of the analytical and numerical studies discussed in the previous sections, the following guidelines for reduced rattle can be established: (i) the first stage should

TABLE 4

Parametric studies for a single stage clutch

(a) *effects of* k_{c1} *and* H_1

($c_{12} = 0$)

k_{c1} (Nm/rad)	H_1 (Nm)	ϕ_s (degrees)	$\bar{\theta}_{12}$ (degrees)	θ_{12rms} (degrees)	L_{β^*} (dB)
5·0	0·00	1·85	1·86	2·09	−7·5
5·0	0·05	1·56	1·56	1·58	−15·3
5·0	0·10	1·28	1·25	1·27	−11·3
5·0	0·15	0·99	0·95	0·97	−8·2
30·0	0·00	0·31	0·31	0·54	1·4
30·0	0·05	0·26	0·26	0·31	−6·1
30·0	0·10	0·21	0·21	0·26	−6·0
30·0	0·15	0·17	0·20	0·25	−2·9

$\bar{\theta}_{12}$ = mean value of $\theta_{12}(t)$.

(b) *effects of* k_{c1} *and* c_{12}

($H_1 = 0$)

k_{c1} (Nm/rad)	c_{12} (Nm/(rad/s))	ϕ_s (degrees)	$\bar{\theta}_{12}$ (degrees)	θ_{12rms} (degrees)	L_{β^*} (dB)
5·0	0·000	1·85	1·86	2·09	−7·5
5·0	0·010	1·85	1·86	1·89	−16·3
5·0	0·050	1·85	1·86	1·87	−17·7
5·0	0·100	1·85	1·86	1·86	−13·5
30·0	0·000	0·31	0·31	0·54	1·4
30·0	0·001	0·31	0·31	0·49	−0·1
30·0	0·010	0·31	0·31	0·38	−5·6
30·0	0·100	0·31	0·31	0·34	−7·3
30·0	0·500	0·31	0·31	0·33	0·6

be designed with low stiffness k_{c1} along with an optimal value of H_1 and c_{12}; (ii) the static balance point ϕ_s should be far removed from the transition points ϕ_{11} and ϕ_{12}, the best choice being $\phi_s = (\phi_{11} + \phi_{12})/2$; (iii) the stiffness transition from k_{c1} to k_{c2} should be as smooth as possible; (iv) the second stage stiffness k_{c2} should be as small as possible while still satisfying the drive torque requirements for the transmission system under running condition; (v) H_2 must be chosen carefully after selecting all other pertinent parameters. Also, it should be noted that the T_{d3} value affects ϕ_s significantly which, in turn, is an important parameter—hence this damper should be chosen judiciously. Since numerous clutch and geared system parameters are involved and the governing equations are non-linear, the computer simulation program for either the overall system or the simplified system must be run to check L_β or L_{β^*}. We should, however, caution that a single clutch design may not be universally applicable; therefore, each case must be analyzed carefully.

10. CONCLUDING REMARKS

This analytical study on neutral gear rattle has made the following contributions to the state of the art. First, numerical errors associated with the non-linear model have been identified. Second, a new rattle criterion has been proposed which can be computed and

TABLE 5

Parametric studies for a dual stage clutch

(a) *transition phenomenon*

($k_{c1}=5{\cdot}0$ Nm/rad, $k_{c2}=3500{\cdot}0$ Nm/rad, $H_1=H_2=0$, $c_{12}=0$, $T_{d3}=-0{\cdot}15$ Nm)

ϕ_{11} (degrees)	ϕ_{12} (degrees)	ϕ_s (degrees)	$\bar{\theta}_{12}$ (degrees)	θ_{12rms} (degrees)	L_{β^*} (dB)
∞	−∞	1·85	1·86	2·09	−7·5
2·0	−∞	1·85	0·58	1·09	10·5
2·0	−0·5	1·85	0·76	1·20	30·1

(b) *effects of k_{c1} and k_{c2}*

($H_1=H_2=0$, $c_{12}=0$, $T_{d3}=-0{\cdot}15$ Nm)

ϕ_{11} (degrees)	ϕ_{12} (degrees)	k_{c1} (Nm/rad)	k_{c2} (Nm/rad)	ϕ_s (degrees)	$\bar{\theta}_{12}$ (degrees)	θ_{12rms} (degrees)	L_{β^*} (dB)
2·0	−0·5	5·0	3500·0	1·85	0·76	1·20	30·1
2·0	−0·5	5·0	2380·0	1·85	0·79	1·18	26·3
1·0	−1·5	30·0	2380·0	0·31	−0·18	0·93	28·3
2·5	0·0	5·0	30·0	1·84	1·62	1·80	−5·8

(c) *effect of T_{d3} on an undamped clutch*

($\phi_{11}=2{\cdot}0°$, $\phi_{11}=-0{\cdot}5°$, $k_{c1}=5{\cdot}0$ Nm/rad, $k_{c2}=3500{\cdot}0$ Nm/rad, $H_1=H_2=0$, $c_{12}=0$)

T_{d3} (Nm)	ϕ_s (degrees)	$\bar{\theta}_{12}$ (degrees)	θ_{12rms} (degrees)	L_{β^*} (dB)
−0·15	1·85	0·76	1·20	30·1
−0·07	1·01	0·75	1·18	29·6
0·00	0·15	0·76	1·23	31·7

(d) *effects of H_1 and H_2*

($\phi_{11}=2{\cdot}0°$, $\phi_{11}=0{\cdot}0°$, $k_{c1}=5{\cdot}0$ Nm/rad, $k_{c2}=3500{\cdot}0$ Nm/rad, $c_{12}=0$, $T_{d3}=-0{\cdot}15$ Nm)

H_1 (Nm)	H_2 (Nm)	ϕ_s (degrees)	$\bar{\theta}_{12}$ (degrees)	θ_{12rms} (degrees)	L_{β^*} (dB)
0·10	0·0	1·28	1·23	1·25	2·1
0·10	0·2	1·28	1·24	1·25	−4·9
0·10	2·0	1·28	1·22	1·25	2·1
0·10	20·0	1·28	1·22	1·25	3·0
0·15	0·0	0·99	0·96	0·98	3·6
0·15	0·2	0·99	0·96	0·98	−6·6
0·15	2·0	0·99	0·95	1·00	4·2
0·15	20·0	0·99	0·96	0·97	0·4

TABLE 5—*continued*

Parametric studies for a dual stage clutch

(e) *effects of transition points and H_2*

($k_{c1}=5\cdot0$ Nm/rad, $k_{c2}=3500\cdot0$ Nm/rad, $H_1=0\cdot1$ Nm, $c_{12}=0$, $T_{d3}=-0\cdot15$ Nm)

ϕ_{11} (degrees)	ϕ_{12} (degrees)	H_2 (Nm)	ϕ_s (degrees)	$\bar{\theta}_{12}$ (degrees)	θ_{12rms} (degrees)	$L_{\beta*}$ (dB)
2·0	0·0	0·0	1·28	1·23	1·25	2·1
2·0	0·0	0·2	1·28	1·24	1·25	−4·9
2·0	0·0	2·0	1·28	1·22	1·25	2·1
2·0	0·0	20·0	1·28	1·22	1·25	3·0
1·5	−0·5	0·0	1·28	0·55	0·85	23·3
1·5	−0·5	0·2	1·28	0·56	0·83	13·1
1·5	−0·5	2·0	1·28	0·62	0·85	10·8
1·5	−0·5	20·0	1·28	0·69	0·84	15·5

(f) *effects of c_{12} and T_{d3}*

($\phi_{11}=2\cdot0°$, $\phi_{12}=0\cdot0°$, $k_{c1}=5\cdot0$ Nm/rad, $k_{c2}=3500\cdot0$ Nm/rad, $H_1=H_2=0$)

c_{12} (Nm/(rad/s))	T_{d3} (Nm)	ϕ_s (degrees)	$\bar{\theta}_{12}$ (degrees)	θ_{12rms} (degrees)	$L_{\beta*}$ (dB)
0·01	−0·15	1·85	0·99	1·26	29·5
0·05	−0·15	1·85	1·05	1·22	13·6
0·10	−0·15	1·85	1·11	1·24	10·0
0·01	−0·09	1·23	1·21	1·25	1·5
0·05	−0·09	1·23	1·22	1·24	1·6
0·10	−0·09	1·23	1·23	1·24	−9·3

(g) *effects of ϕ_{11} and c_{12}*

($k_{c1}=5\cdot0$ Nm/rad, $k_{c2}=3500\cdot0$ Nm/rad, $H_1=H_2=0$, $T_{d3}=-0\cdot09$ Nm)

ϕ_{11} (degrees)	ϕ_{12} (degrees)	c_{12} (Nm/(rad/s))	ϕ_s (degrees)	$\bar{\theta}_{12}$ (degrees)	θ_{12rms} (degrees)	$L_{\beta*}$ (dB)
2·0	0·0	0·01	1·23	1·21	1·25	1·5
2·0	0·0	0·05	1·23	1·22	1·24	1·6
2·0	0·0	0·10	0·23	1·23	1·24	−9·3
1·5	0·0	0·01	1·23	0·76	0·95	27·2
1·5	0·0	0·05	1·23	0·75	0·95	27·4
1·5	0·0	0·10	1·23	1·20	1·22	1·6

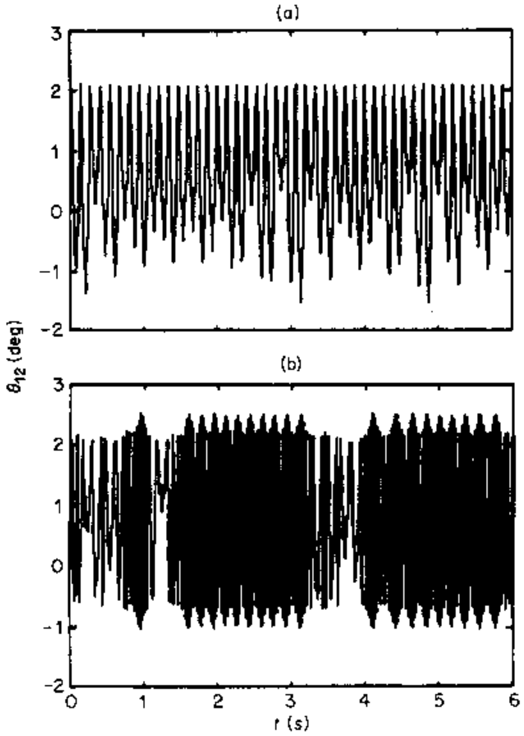

Figure 12. Results for the dual stage clutch. (a) Stiffness transition at only one side ($\phi_{11} = 2 \cdot 0°$, $\phi_{12} = -\infty$), $L^*_\beta = 10 \cdot 5$ (dB); (b) stiffness transition at both sides ($\phi_{11} = 2 \cdot 0°$, $\phi_{12} = -0 \cdot 5°$), $L^*_\beta = 30 \cdot 1$ (dB).

utilized efficiently and reliably. Third, a simplified physical model of the rattle problem has been given and its application has been demonstrated. Fourth, systematic design of the clutch and various relevant issues such as the balance points and transition phenomenon have been discussed. Perhaps of fundamental importance has been the presentation of analytical details and clarification of several aspects of the neutral rattle problem, which should benefit both designers and researchers.

Some of the issues raised by this study, including the numerical difficulties, are essentially related to the nature of gear backlash and clutch nonlinearities. Ongoing research work in this area is focusing on the following specific topics: development of approximate analytical solutions for the gear pair and the flywheel-clutch subsystem, extension of the current work to the study of gear noise and vibration problems under the driving conditions, examination of various mathematical models including the order of the dynamic system and the composition of the forcing function, and measurements on a laboratory rattle test stand. These issues will be discussed in future papers.

ACKNOWLEDGMENT

The authors wish to express their gratitude to the Chrysler Corporation for supporting this study. We also thank Jim Frey, Tom Brown and Don Houser for their assistance.

REFERENCES

1. T. SAKAI, Y. DOI, M. YAMAMOTO, T. OGASAWARA and M. NARITA 1981 *SAE Paper No.* 810773. Theoretical and experimental analysis of rattling noise of automotive gearbox.

2. S. OHNUMA, Y. SHIGETARO, I. MINEICHI and T. FUJIMOTO 1985 *SAE Paper No.* 850979. Research on idling rattle of manual transmission.
3. T. FUJIMOTO, Y. CHIKATANI and J. KOJIMA 1987 *SAE Paper No.* 870395. Reduction of idling rattle in manual transmission.
4. R. L. SEAMAN, C. E. JOHNSON and R. F. HAMILTON 1984 *SAE Paper No.* 841686. Component inertial effects on transmission design.
5. W. REIK 1986 *LUK Company Report.* Torsional vibrations and transmission noise.
6. L. F. SCHULTE 1986 *LUK Company Report.* Dual mass flywheel.
7. A. SEBULKE 1987 *SAE Paper No.* 870394. The two-mass flywheel—a torsional vibration damper for the power train of passenger cars—state of the art and further technical development.
8. H. J. DREXL 1987 *SAE Paper No.* 870393. Torsional dampers and alternative systems to reduce driveline vibration.
9. R. A. FRANTZ 1984 *SAE Paper No.* 841195. Cam-driven member assembly—improvements in clutch neutral rattle performance.
10. J. L. HEDGES and K. J. BUTLER 1979 *Institution of Mechanical Engineers Paper* C121/79. A "CAD" system for the analysis of the vehicle driveline noise.
11. G. L. FUDALA, T. C. ENGLE and A. V. KARVELIS 1987 *SAE Paper No.* 870396. *A system approach to reducing gear rattle.*
12. R. J. COMPARIN 1987 *Ph.D. Dissertation Proposal, the Ohio State University.*
13. F. S. TSE, I. E. MORSE and R. T. HINKLE 1978 *Mechanical Vibrations Theory and Applications.* Boston: Allyn and Bacon. See pp. 43 and 95.